

Stiffness modeling of a family of 6-DoF parallel mechanisms with three limbs based on screw theory[†]

Bing Li^{1,*}, Hongjian Yu¹, Zongquan Deng², Xiaojun Yang¹ and Hong Hu¹

¹Shenzhen Graduate School, Harbin Institute of Technology, P. R. China

²School of Mechatronics Engineering, Harbin Institute of Technology, P. R. China

(Manuscript Received October 28, 2008; Revised August 19, 2009; Accepted October 8, 2009)

Abstract

The stiffness modeling of a family of six degrees of freedom (DoF) parallel mechanisms with configurations of 3-RUPU is presented. The mobility of the mechanisms is firstly analyzed, and then the stiffness analysis and modeling of the family of mechanisms is developed by a novel screw-theory based method. The method employs screw theory as a tool for force analysis and deformation analysis. Based on the developed stiffness model, two global flexibility indices, which refer to the maximum and minimum singular values of compliance matrix, are introduced to evaluate the compliance of parallel mechanisms. Finally, a case study is presented to demonstrate the effectiveness of the method in analyzing and evaluating the stiffness behavior of the presented parallel mechanisms.

Keywords: Stiffness modeling; Screw theory; Parallel mechanism; Flexibility index

1. Introduction

The design of parallel mechanisms is a process in which many criteria, such as the workspace, dexterity and stiffness, etc. have to be considered. The global stiffness and workspace of the parallel mechanisms vary with the configuration of the assembled parallel kinematic chains [1-3]. In fact, there is always a tradeoff between stiffness and workspace in the design of such mechanisms. The family of parallel mechanisms based on Gough-Stewart platform is increasingly being used to construct devices for various fields [4-5]. But their complicated structure and interference between the kinematic chains greatly reduce the workspace volume. To solve this issue, efforts have been made by several researchers who proposed structures of 6-DoF parallel mechanisms with three limbs [6-8]. We also made our attempts to present a family of parallel mechanisms with configuration of 3-RUPU (R, U, P respectively refers to revolute, universal and prismatic joint) [9]. The mechanisms are characterized by the presence of a mobile platform connected to fixed base by three identical limbs with configuration of RUPU; the 3D model of a typical 3-RUPU mechanism is shown in Fig. 1. There exist two actuations in each limb, a swing link turning in base plane and an extendible link supporting the platform. Both the platform and the

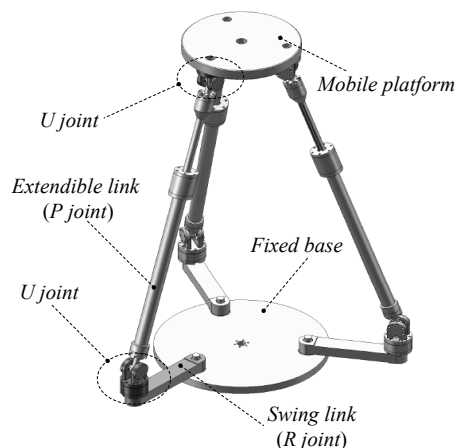


Fig. 1. 3D model of a typical 3-RUPU parallel mechanism.

swing link are connected with the extendible link by U joints. According to different schemes of the axes of U joints as shown in Table 1, the geometry of RUPU kinematic chains can be classified into the following 16 different types, as shown in Table 2.

The stiffness and strength of the parallel mechanisms have direct effects on the operational precision of the mechanism. In this paper the main focus is on the stiffness modeling of the parallel mechanisms, which establishes the relationship between the deformation and payload on the manipulator. The main issue in stiffness modeling is the establishment of a rela-

[†] This paper was recommended for publication in revised form by Associate Editor Jong Hyeon Park

*Corresponding author. Tel.: +86 755 26033485, Fax.: +86 755 26033485

E-mail address: libing.sgs@hit.edu.cn

© KSME & Springer 2010

Table 1. Different schemes of U joint.






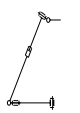
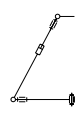


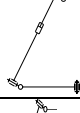
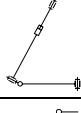
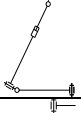
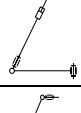
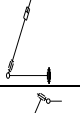
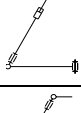
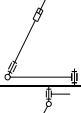
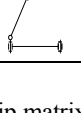
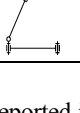
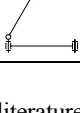
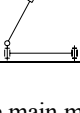
	
(A)	(B)
	
(C)	(D)

Table 2. Schematic diagram of the RUPU kinematic chains.

	A	B	C	D
A				
B				
C				
D				

tionship matrix. As reported in the literature, three main methods have been used to derive the stiffness model of parallel manipulators [10]; these methods are based on the calculation of the Jacobian matrix [11-15]; the finite element analysis (FEA) [16, 17] and the matrix structural analysis (MSA) [10, 18-21]. For the three methods, the Jacobian matrix method utilizes the duality between force and velocity, associated with the Jacobian matrix, to formulate a generalized stiffness matrix [14]; the uses of FE models are reliable, and can be calculated by FEA software; the methods based on MSA are simple and easy for computational implementation. These models are well adapted to validate analytical models or some experimental results, but there still exist some drawbacks. For example, the methods based on the calculation of the Jacobian matrix and MSA are on the basis of force analysis and deformation analysis; there are always some kind of predigestions and presumptions in the analysis process, especially to the deformation of the links, i.e., the existence and direction of the deformation are generally identified by observation for simplicity purpose; the method based on FEA involves tedious remeshing procedure and the process is also time-consuming.

This paper aims at developing a systematic and analytical method for stiffness modeling of parallel mechanisms based on screw theory. The method employs screw theory as a tool for force analysis and deformation analysis. According to screw theory, the driving forces and deformations of kine-

matic chains are described by effective screws and deformation screws. The existence of the deformation of each kinematic chain is identified in terms of the relationship between effective screw and deformation screw, and then the stiffness model of the mechanism can be constructed by virtue of the duality of kinematics and statics; the deformation of component links is taken as infinitesimal input and the output of the mobile platform is the corresponding deformation of mechanism.

This paper is organized as follows: the mobility analysis of the family of 3-RUPU mechanisms is presented in section 2; the stiffness analysis and modeling of mechanism are conducted in section 3; in section 4 the maximum and minimum singular value of compliance matrix as are employed as flexibility indices to represent the maximum and minimum variation of the platform under unit wrench; a case study is presented in section 5; the last section is the conclusions.

2. Mobility analysis of mechanisms

As illustrated in Table 2, when the swing link and extendible link are connected by joint A or C (shown in Table 1), the two links will always be coplanar and form a linkage plane; especially when the two links are connected by joint C, the linkage plane will be vertical to the base all along. Otherwise, when the links are connected by joint B or D, the two links will not be coplanar with the movement of the mechanism, which makes the kinematic relations between the links more complicated. When the links are connected by joint C, four kinematic chains C-A, C-B, C-C, C-D can be obtained as shown in the third row of Table 2. Among the four kinematic chains both the chains of C-A and C-D are equivalent to the RRPS kinematic chain, as shown in Fig. 2 the RRPS kinematic chain has a geometric feature, the projection of O_iP_i is always superposed with O_iB_i ; thus the inverse kinematics of mechanism constructed by the chains of C-A and C-D can be simplified. In this paper the mechanism constructed by the kinematic chain C-A is used as examples for later analysis.

Based on screw theory the mobility of the mechanism constructed by chain C-A is analyzed as follows: to facilitate the analysis a local Cartesian frame $B_i\{x_i y_i z_i\}$ with B_i as the origin is set up as shown in Fig. 3, the x_i -axis of the frame is along the elongation line of the swing link, the y_i -axis is superposed with axis S_{i2} , and the z_i -axis satisfies the right hand rule. So the frame plane $x_i z_i$ will be always superposed with plane $P_iB_iO_i$. The instantaneous twist system of a single kinematic chain C-A can be expressed as follows:

Where $S_{ij}, j=1, 2, \dots, 6$ is the j th joint screw of the i th chain; Φ_1 refers to the included angle between B_iP_i and O_iB_i ; Φ_2 stands for the turn angle of axis S_{i3} ; Φ_3 represents the included angle between PP_i and B_iP_i ; l_s and l_e represent the lengths of swing link and extendible link.

The mechanism is actuated by both the swing link and extendible link, and the corresponding active screws are S_{i1} and S_{i4} . If the active screw S_{i1} or S_{i4} is fixed, the rest joints of the

$$\begin{Bmatrix} \mathcal{S}_{i1} \\ \mathcal{S}_{i2} \\ \mathcal{S}_{i3} \\ \mathcal{S}_{i4} \\ \mathcal{S}_{i5} \\ \mathcal{S}_{i6} \end{Bmatrix} = \begin{Bmatrix} 0 & 0 & 1; & 0 & l_{si} & 0 \\ 0 & 1 & 0; & 0 & 0 & 0 \\ -\cos \phi_1 & 0 & \sin \phi_1; & 0 & 0 & 0 \\ 0 & 0 & 0; & -\cos \phi_1 & 0 & \sin \phi_1 \\ -\sin \phi_1 \sin \phi_2 & \cos \phi_2 & -\cos \phi_1 \sin \phi_2; & -l_{ei} \sin \phi_1 \cos \phi_2 & -l_{ei} \sin \phi_2 & -l_{ei} \cos \phi_1 \cos \phi_2 \\ \cos \phi_1 \cos \phi_3 + \sin \phi_1 \cos \phi_2 \sin \phi_3 & \sin \phi_2 \sin \phi_3 & -\sin \phi_1 \cos \phi_3 + \cos \phi_1 \cos \phi_2 \sin \phi_3; & -l_{ei} \sin \phi_1 \sin \phi_2 \sin \phi_3 & l_{ei} \cos \phi_2 \sin \phi_3 & -l_{ei} \cos \phi_1 \sin \phi_2 \sin \phi_3 \end{Bmatrix} \quad (1)$$

kinematic chain form a five dimensional twist system, where the reciprocal screw represents the driving force exerted by the limb, namely, *effective screw* to the active joint. The effective screws of the *i*th kinematic chain are very important to the following analysis; the screws form a 2-dimensional screw system $\{\mathcal{S}^r\}$, as described in Eq. (2), the acting directions and points of the effective screws are depicted as the solid arrows in Fig. 3.

$$\{\mathcal{S}_i^r\} = \begin{Bmatrix} \mathcal{S}_{i1}^r \\ \mathcal{S}_{i2}^r \end{Bmatrix} = \begin{Bmatrix} -\cos \phi_1 & 0 & \sin \phi_1; & 0 & 0 & 0 \\ 0 & 1 & 0; & -l_{ei} \sin \phi_1 & 0 & -l_{ei} \cos \phi_1 \end{Bmatrix} \quad (2)$$

According to Eq. (1) the kinematic joints of the C-A chain are linearly independent, and can form a 6 dimensional twist system except for two singular cases of each limb:

- (1) $\Phi_3=0$, refers to axis \mathcal{S}_{i3} being coaxial with \mathcal{S}_{i6} ;
- (2) $l_{si}=l_{ei}\cos\Phi_1$, refers to the projection of point P_i superposed with point O_i .

Simultaneously, the effective screws of the three limbs can construct a 6-dimensional effective screw system, except for the above two singular cases. Based on the above analysis it shows that the parallel mechanism constructed by 3 kinematic chains of C-A can implement 6 DoFs and all the 6 DoFs can be driven by 3 swing links and 3 extendible links.

3. Stiffness analysis and modeling

The compliance of a parallel mechanism at a given point within its workspace can be characterized by its compliance matrix. The compliance matrix represents the mechanism's ability of resisting the applied forces and torques. As shown in Eq. (3) the generalized compliance matrix C represents the relationship between the forces and torques applied on the platform and the corresponding linear and angular displacements.

$$\delta X = C \cdot w \quad (3)$$

Where w is the vector representing the external wrench acting on the mobile platform, it's the general designation of the generalized forces and torques, δX is the vector of the linear and angular deformation of the mobile platform, i.e. the infinitesimal displacement of the platform relative to the base.

Based on the superposition method, the displacement of the platform is the effective superposition of the deformation of all kinematic chains. Deformation of the mobile platform can be described with a linear combination of the subchain defor-

mation and joints motion. If the relationship is expressed in screw form, and taking the reciprocal product of both sides with effective screw \mathcal{S}_i^r , the matrix presentation can be obtained (detailed modeling process is conducted in Section 3.3).

$$\delta X = H \cdot \delta q \quad (4)$$

Where H represents the *incidence matrix*, which is the inverse matrix of Jacobian matrix that relates the infinitesimal motion between the subchains and the mobile platform, δq is the vector representing infinitesimal motion of the subchains. The infinitesimal motion of the subchains is referred to as the component deformation of the sub-serial chains. The component deformation will induce forces, which are called the

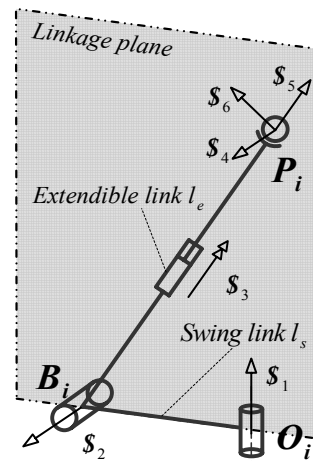


Fig. 2. Equivalent kinematic chain RRPS.

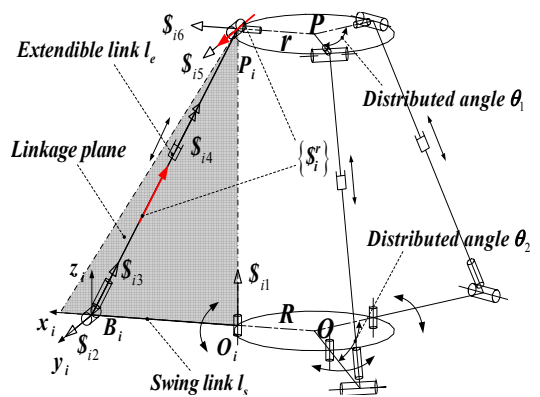


Fig. 3. Schematic diagram of 3-RUPU parallel mechanisms.

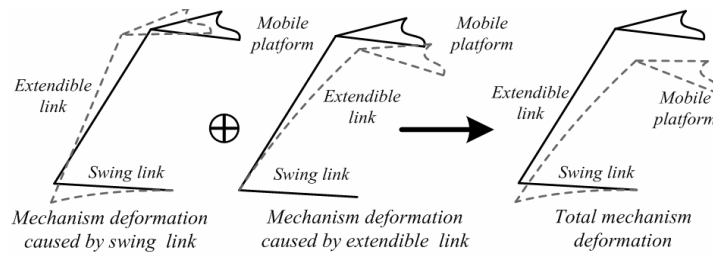


Fig. 4. Schematic diagram of mechanism deformation caused by component link deformations.

branch forces in the subchains.

By virtue of the duality of kinematics and statics, the forces and moments applied on the platform under static conditions are related to the forces or moments required in the subchain to maintain the equilibrium as shown in Eq. (5).

$$f = \mathbf{H}^T \cdot w \tag{5}$$

Where f stands for the vector of branch forces in the subchain; with consideration of the local stiffness in the subchains, the relationship between the branch forces and branch deformation can be given as:

$$\delta q = \mathbf{h} \cdot f \tag{6}$$

Substituting Eq. (5) and Eq. (6) into Eq. (4) yields,

$$\delta X = \mathbf{HhH}^T \cdot w \tag{7}$$

Combining Eq. (7) the generalized compliance matrix can be given as:

$$\mathbf{C} = \mathbf{HhH}^T \tag{8}$$

By using the superposition method into Eq. (3), the following mechanism deformation can be induced,

$$\delta X_e = \mathbf{C}_e \cdot w, \quad \delta X_s = \mathbf{C}_s \cdot w \tag{9}$$

Where, subscripts s and e indicate the deformations due to linear and angular deformations on swing and extendible links, respectively. Fig. 4 illustrates the deformation superposition of component links, so the total deformation of whole mechanism can be simplified as Eq. (10); the deformation and stiffness modeling of extendible and swing link will be developed in the following section.

$$\delta X = \delta X_e + \delta X_s \tag{10}$$

This leads to the following compliance model:

$$\delta X = \mathbf{C}_G \cdot w \tag{11}$$

In Eq. (11) the global generalized compliance matrix \mathbf{C}_G is given as:

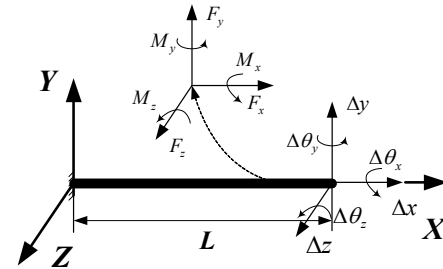


Fig. 5. Cantilever beam element in link coordinate system.

$$\mathbf{C}_G = \mathbf{C}_e + \mathbf{C}_s \tag{12}$$

Where,

$$\mathbf{C}_e = \mathbf{H}_e \mathbf{h}_e \mathbf{H}_e^T, \quad \mathbf{C}_s = \mathbf{H}_s \mathbf{h}_s \mathbf{H}_s^T \tag{13}$$

3.1 Modeling of component link

The link of parallel mechanism can be considered as a cantilever beam for its large ratio of length to diameter. The flexibility of the mechanism can be calculated by the superposition method, which means that the displacement of the platform is the effective superposition of the deformation of kinematic chains. The link deformation can be considered as the relative displacement between the two extremity nodes; the component link of the chain can be considered as a cantilever beam as shown in Fig. 5.

According to material mechanics and screw theory, there exists a 6-dimensional force screw system on the free end of the cantilever beam as depicted in Fig. 5; the force screw system $\{F\}$ with respect to the link coordinate system can be expressed as:

$$\{F\} = \begin{Bmatrix} \overline{F}_x \\ \overline{F}_y \\ \overline{F}_z \\ \overline{M}_x \\ \overline{M}_y \\ \overline{M}_z \end{Bmatrix} = \begin{bmatrix} 1 & 0 & 0; & 0 & 0 & 0 \\ 0 & 1 & 0; & 0 & 0 & L \\ 0 & 0 & 1; & 0 & -L & 0 \\ 0 & 0 & 0; & 1 & 0 & 0 \\ 0 & 0 & 0; & 0 & 1 & 0 \\ 0 & 0 & 0; & 0 & 0 & 1 \end{bmatrix}_{6 \times 6} \tag{14}$$

Correspondingly, there are three kinds of deformation: tensile deformation, torsional deformation and bending deformation on the free end. The screw presentation of deformation in

link coordinate system is shown in Table 3; the matrix form of the deformation screw system can be represented as shown in Eq. (15).

$$\begin{bmatrix} \overline{S}_{ux}^d \\ \overline{S}_{\theta_x}^d \\ \overline{S}_{uy}^d \\ \overline{S}_{\theta_z}^d \\ \overline{S}_{uz}^d \\ \overline{S}_{\theta_y}^d \end{bmatrix} = \begin{bmatrix} 0 & 0 & 0; & 1 & 0 & 0 \\ \hline 1 & 0 & 0; & 0 & 0 & 0 \\ 0 & 0 & 0; & 0 & 1 & 0 \\ \hline 0 & 0 & 1; & 0 & -L & 0 \\ 0 & 0 & 0; & 0 & 0 & 1 \\ \hline 0 & 1 & 0; & 0 & 0 & L \end{bmatrix}_{6 \times 6} \quad (15)$$

The deformation screw is caused by the force screw if the reciprocal product of the two screws is nonzero. Especially, the bending deformation is a kind of compounded deformation, including the nodal displacement and sectional rotation, the reciprocal product of force screw and bending deformation screw is a dyadic array. When the array has one nonzero element ($\{0 \ 1\}^T, \{1 \ 0\}^T$), the deformation screw can be generated upon the application of force screw. According to [22], the compliance model of the link can be established via compliance equation, as shown in Eq. (16). Where $\{\overline{u}_x \ \overline{u}_y \ \overline{u}_z; \overline{\theta}_x \ \overline{\theta}_y \ \overline{\theta}_z\}$ represents the nodal displacement vector at the free end of the link, and $\{\overline{F}_x \ \overline{F}_y \ \overline{F}_z; \overline{M}_x \ \overline{M}_y \ \overline{M}_z\}$ represents the nodal load at the same node. E and G are respectively the Young's and shear modulus, A is the sectional area, L is the length of link, I is the moment of inertia, J is the polar moment of inertia.

$$\begin{bmatrix} \overline{u}_x \\ \overline{\theta}_x \\ \overline{u}_y \\ \overline{\theta}_z \\ \overline{u}_z \\ \overline{\theta}_y \end{bmatrix} = \begin{bmatrix} \frac{L}{EA} & 0 & 0 & 0 & 0 & 0 \\ 0 & 0 & 0 & \frac{L}{GJ} & 0 & 0 \\ \hline 0 & \frac{L^3}{3EI} & 0 & 0 & 0 & \frac{L^2}{2EI} \\ 0 & \frac{L^2}{2EI} & 0 & 0 & 0 & \frac{L}{EI} \\ \hline 0 & 0 & \frac{L^3}{3EI} & 0 & -\frac{L^2}{2EI} & 0 \\ 0 & 0 & -\frac{L^2}{2EI} & 0 & \frac{L}{EI} & 0 \end{bmatrix}_{6 \times 6} \begin{bmatrix} \overline{F}_x \\ \overline{F}_y \\ \overline{F}_z \\ \overline{M}_x \\ \overline{M}_y \\ \overline{M}_z \end{bmatrix} \quad (16)$$

3.2 Deformation analysis of component link

Due to the complexity in structure of the parallel mechanism, the deformation analysis to the subchains includes the existence check of the deformation and the decoupling of the

deformation. The existence of the deformation can be carried out by solving the reciprocal product of the deformation screw S^d and the effective screw S_i^r , which is reciprocal to all the twists of the subchain with the exception of the active one. The existence condition is that the reciprocal product of the two screws is nonzero; the physical meaning is that the applied work of branch force on the existed deformations is nonzero, so the relationship can be considered as follows:

$$S_i^r \circ S^d \neq \{0\} \quad (17)$$

As illustrated in Fig. 6, the analysis is conducted in the local coordinate system $B_r\{x_i \ y_i \ z_i\}$, and the deformations of the component links are respectively represented by deformation screw systems in swing link coordinate system $O_r\{x_{si} \ y_{si} \ z_{si}\}$ and extendible link coordinate system $B_r\{x_{ei} \ y_{ei} \ z_{ei}\}$. According to the former analysis, the compliance of the mechanism is the superposition of the compliance of the extendible link and the swing link. Before the superposition of two parts, deformation analyses of two links are separated; during the deformation analysis of one link, the other one should be taken as rigid body. The deformation analysis of the subchain is conducted as follows.

3.2.1 Extendible link deformation analysis

Taking the extendible link as a cantilever beam element, then its deformation screw system in extendible link coordinate system $B_r\{x_{ei} \ y_{ei} \ z_{ei}\}$ (as depicted in Fig. 6), can be expressed as Eq. (15). Considering the whole mechanism, the deformation screw system of each extendible link should be transformed into the local coordinate system as:

$$S_{ei}^d = \begin{bmatrix} \overline{S}_{uexi}^d \\ \overline{S}_{\theta_xi}^d \\ \overline{S}_{ueyi}^d \\ \overline{S}_{\theta_zi}^d \\ \overline{S}_{uezi}^d \\ \overline{S}_{\theta_yi}^d \end{bmatrix} = \begin{bmatrix} 0 & 0 & 0; & -\cos\phi_1 & 0 & \sin\phi_1 \\ \hline -\cos\phi_1 & 0 & \sin\phi_1; & 0 & 0 & 0 \\ 0 & 0 & 0; & -\sin\phi_1 & 0 & -\cos\phi_1 \\ \hline 0 & 1 & 0; & -l_{ei}\sin\phi_1 & 0 & -l_{ei}\cos\phi_1 \\ 0 & 0 & 0; & 0 & 1 & 0 \\ \hline \sin\phi_1 & 0 & \cos\phi_1; & 0 & l_{ei} & 0 \end{bmatrix} \quad (18)$$

The reciprocal product of effective screw in Eq. (2) and deformation screw in Eq. (18) can be given as:

$$\begin{aligned} S_{i1}^r \circ S_{ei}^d &= \{1\} \ \{0\} \ \{0 \ 0\} \ \{0 \ 0\}^T \\ S_{i2}^r \circ S_{ei}^d &= \{0\} \ \{0\} \ \{0 \ 0\} \ \{1 \ 0\}^T \end{aligned} \quad (19)$$

$$\begin{bmatrix} S_{ei}^d \\ S_i \end{bmatrix} = \begin{bmatrix} 0 & 0 & 0; & -\cos\phi_1 & 0 & \sin\phi_1 \\ \hline 0 & 0 & 0; & 0 & 1 & 0 \\ \sin\phi_1 & 0 & \cos\phi_1; & 0 & l_{ei} & 0 \\ \hline 0 & 1 & 0; & 0 & 0 & 0 \\ -\cos\phi_1 & 0 & \sin\phi_1; & 0 & 0 & 0 \\ \hline -\sin\phi_1\sin\phi_2 & \cos\phi_2 & -\cos\phi_1\sin\phi_2; & -l_{ei}\sin\phi_1\cos\phi_2 & -l_{ei}\sin\phi_2 & -l_{ei}\cos\phi_1\cos\phi_2 \\ \cos\phi_1\cos\phi_3 + \sin\phi_2\sin\phi_3 & -\sin\phi_1\cos\phi_3 + \sin\phi_2\sin\phi_3 & -\sin\phi_1\sin\phi_2\sin\phi_3; & -l_{ei}\sin\phi_1\sin\phi_2\sin\phi_3 & l_{ei}\cos\phi_2\sin\phi_3 & -l_{ei}\cos\phi_1\sin\phi_2\sin\phi_3 \\ \sin\phi_1\cos\phi_2\sin\phi_3 & \cos\phi_1\cos\phi_2\sin\phi_3; & & & & \end{bmatrix} \quad (20)$$

Table 3. Screw presentation of cantilever beam deformation in link coordinate system.

\bar{S}_{ux}^d	$[0 \ 0 \ 0; \ 1 \ 0 \ 0]$	Tensile deformation screw in x direction
$\bar{S}_{\theta x}^d$	$[1 \ 0 \ 0; \ 0 \ 0 \ 0]$	Torsional deformation screw in x direction
$\begin{Bmatrix} \bar{S}_{uy}^d \\ \bar{S}_{\theta z}^d \end{Bmatrix}$	$\begin{bmatrix} 0 & 0 & 0; & 0 & 1 & 0 \\ 0 & 0 & 1; & 0 & -L & 0 \end{bmatrix}$	Bending deformation screw in z direction
$\begin{Bmatrix} \bar{S}_{uz}^d \\ \bar{S}_{\theta y}^d \end{Bmatrix}$	$\begin{bmatrix} 0 & 0 & 0; & 0 & 0 & 1 \\ 0 & 1 & 0; & 0 & 0 & L \end{bmatrix}$	Bending deformation screw in y direction

From Eq. (19), the deformations occurring on the extendible link are tensile and bending deformation. The combined screw system composed of deformations screw and joint screw (except the active screw) can be expressed as:

By simplification of the combined screw system, we can get that the joint screws and sectional rotation screws are linearly dependent, which means the effect of sectional rotation deformation is reduced.

From Eq. (16) the local compliance function can be given as:

$$\begin{bmatrix} \bar{u}_{exi} \\ \bar{u}_{ezi} \end{bmatrix} = \begin{bmatrix} \frac{l_{ei}}{EA} \\ \frac{l_{ei}^3}{3EI} \end{bmatrix} \begin{bmatrix} f_{e1} \\ f_{e2} \end{bmatrix} \quad [h_{ei}]_{2 \times 2} = \begin{bmatrix} \frac{l_{ei}}{EA} & \\ & \frac{l_{ei}^3}{3EI} \end{bmatrix} \quad (21)$$

Where, $[\bar{u}_{exi} \ \bar{u}_{ezi}]^T$ and $[f_{e1} \ f_{e2}]^T$ represent the vectors of deformation and support reactions of the i th extendible link respectively, and $[h_{ei}]_{2 \times 2}$ is the stiffness matrix of the i th link.

3.2.2 Swing link Deformation Analysis

Similarly, taking the swing link as a cantilever beam element, then its deformation screw system in swing link coordinate system $O_r\{x_{si} \ y_{si} \ z_{si}\}$ (as depicted in Fig. 6), can be expressed as Eq. (15). Considering the whole mechanism, the deformation screw system of each swing link should be transformed into the local coordinate system, which yields,

$$\begin{Bmatrix} S_{si}^d \\ S_i^r \end{Bmatrix} = \begin{bmatrix} 0 & 0 & 0; & 1 & 0 & 0 \\ 1 & 0 & 0; & 0 & 0 & 0 \\ 0 & 0 & 0; & 0 & 1 & 0 \\ 0 & 0 & 0 & 1; & 0 & 0 \\ 0 & 0 & 0; & 0 & 0 & 1 \\ 0 & 1 & 0; & 0 & 0 & 0 \\ 0 & 1 & 0; & 0 & 0 & 0 \\ -\cos\phi_1 & 0 & \sin\phi_1; & 0 & 0 & 0 \\ -\sin\phi_1\sin\phi_2 & \cos\phi_2 & -\cos\phi_1\sin\phi_2; & -l_{ei}\sin\phi_1\cos\phi_2 & -l_{ei}\sin\phi_2 & -l_{ei}\cos\phi_1\cos\phi_2 \\ \cos\phi_1\cos\phi_3 + \sin\phi_1\cos\phi_2\sin\phi_3 & \sin\phi_2\sin\phi_3 & -\sin\phi_1\cos\phi_3 + \cos\phi_1\cos\phi_2\sin\phi_3; & -l_{ei}\sin\phi_1\sin\phi_2\sin\phi_3 & l_{ei}\cos\phi_2\sin\phi_3 & -l_{ei}\cos\phi_1\sin\phi_2\sin\phi_3 \end{bmatrix} \quad (24)$$

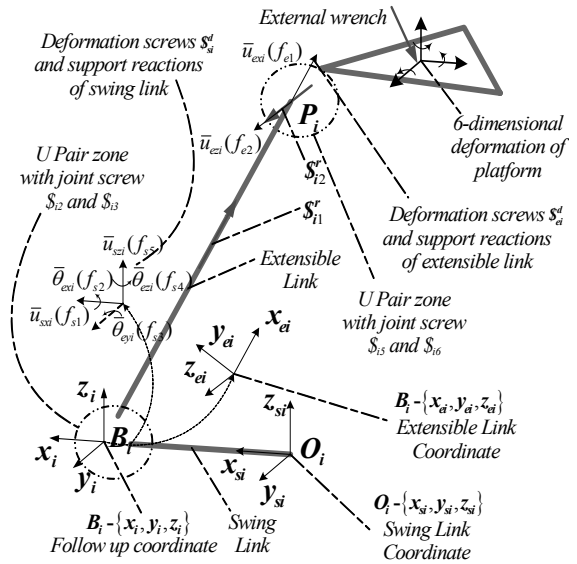


Fig. 6. Schematic of coordinate and screw system of subchain.

$$S_{si}^d = \begin{Bmatrix} S_{usxi}^d \\ S_{\theta sxi}^d \\ S_{usyi}^d \\ S_{\theta syi}^d \\ S_{uszi}^d \\ S_{\theta syi}^d \end{Bmatrix} = \begin{bmatrix} 0 & 0 & 0; & 1 & 0 & 0 \\ 1 & 0 & 0; & 0 & 0 & 0 \\ 0 & 0 & 0; & 0 & 1 & 0 \\ 0 & 0 & 1; & 0 & 0 & 0 \\ 0 & 0 & 0; & 0 & 0 & 1 \\ 0 & 1 & 0; & 0 & 0 & 0 \end{bmatrix} \quad (22)$$

Then the reciprocal product of effective screw and deformation screw can be given as shown in Eq. (23):

$$\begin{aligned} S_{i1}^r \circ S_{si}^d &= \{-\cos\phi_{i1} \ \{0\} \ \{0 \ 0\} \ \{\sin\phi_{i1} \ 0\}\}^T \\ S_{i2}^r \circ S_{si}^d &= \{\{0\} \ \{-l_{ei}\sin\phi_{i1}\} \ \{1 \ -l_{ei}\cos\phi_{i1}\} \ \{0 \ 0\}\}^T \end{aligned} \quad (23)$$

From Eq. (23), there is a 6-dimensional deformation system occurring on the swing link. The compound screw system composed of deformation screw and joint screw (except the active screw) can be expressed as shown in Eq. (24).

By simplification of the compound screw system, we can easily get that the effect of sectional rotation deformation coaxial with the S_{i3} joint is reduced.

From Eq. (16) the local compliance function can be given as:

$$\begin{bmatrix} \bar{u}_{sxi} \\ \bar{\theta}_{sxi} \\ \bar{u}_{sxi} \\ \bar{\theta}_{sxi} \\ \bar{u}_{sxi} \end{bmatrix} = \begin{bmatrix} \frac{l_{si}}{EA} & 0 & 0 & 0 & 0 \\ 0 & 0 & 0 & \frac{l_{si}}{GJ} & 0 \\ 0 & \frac{l_{si}^3}{3EI} & 0 & 0 & \frac{l_{si}^2}{2EI} \\ 0 & \frac{l_{si}^2}{2EI} & 0 & 0 & \frac{l_{si}}{EI} \\ 0 & 0 & \frac{l_{si}^3}{3EI} & 0 & 0 \end{bmatrix} \begin{bmatrix} f_{s1} \\ f_{s2} \\ f_{s3} \\ f_{s4} \\ f_{s5} \end{bmatrix}$$

$$[\mathbf{h}_{si}]_{5 \times 5} = \begin{bmatrix} \frac{l_{si}}{EA} & 0 & 0 & 0 & 0 \\ 0 & 0 & 0 & \frac{l_{si}}{GJ} & 0 \\ 0 & \frac{l_{si}^3}{3EI} & 0 & 0 & \frac{l_{si}^2}{2EI} \\ 0 & \frac{l_{si}^2}{2EI} & 0 & 0 & \frac{l_{si}}{EI} \\ 0 & 0 & \frac{l_{si}^3}{3EI} & 0 & 0 \end{bmatrix} \quad (25)$$

Where, $[\bar{u}_{sxi} \ \bar{\theta}_{sxi} \ \bar{u}_{sxi} \ \bar{\theta}_{sxi} \ \bar{u}_{sxi}]^T$ and $[f_{s1} \ f_{s2} \ f_{s3} \ f_{s4} \ f_{s5}]^T$ respectively represent the vectors of deformation and support reactions of the i th swing link, and $[\mathbf{h}_{si}]_{5 \times 5}$ is the stiffness matrix of the i th link.

3.3 Stiffness modeling of mechanism

The deformation of the mobile platform δX equals to the combined deformation of the i th kinematic chain δX_i , which can be described with a linear combination of the subchain deformation and infinitesimal motions of the passive joints; the screw expression can be given as:

$$\{\delta X_i\} = \sum_{j=2,3}^{5,6} q_{ij} S_{ij} + \sum_{k=1}^m d_{ik} S_{ik}^d \quad (26)$$

Where S_{ij} represents the unit screw including the position and direction of the joint screw associated with the passive kinematic joint of the i th subchain, $j=2, 3, 5, 6$; q_{ij} stands for its amplitude; S_{ik}^d represents unit deformation screw occurring on the component links, and d_{ik} stands for its amplitude, m refers to the number of deformations occurring on the component links.

3.3.1 Extendible link

When considering the deformations of the extendible links only, from Eq. (26) the deformation equation of extendible links can be expressed as:

$$\{\delta X_e\} = \sum_{j=2,3}^{5,6} q_{ij} S_{ij} + \sum_{k=1}^2 d_{eik} S_{eik}^d \quad \text{for } i=1, 2, 3 \quad (27)$$

Taking the reciprocal product of both sides of Eq. (27) with S_i^r , yields,

$$S_i^r \circ \{\delta X_e\} = \begin{bmatrix} S_{i1}^r \circ S_{uex1}^d \\ S_{i2}^r \circ S_{uezi}^d \end{bmatrix} \begin{bmatrix} \bar{u}_{exi} \\ \bar{u}_{ezi} \end{bmatrix} \quad (28)$$

Eq. (28) can be written in matrix form as:

$$\begin{bmatrix} S_1^r \\ S_2^r \\ S_3^r \end{bmatrix} \circ \{\delta X_e\} = \begin{bmatrix} S_{11}^r \circ S_{uex1}^d & & & \\ & S_{12}^r \circ S_{uez1}^d & & \\ & & S_{21}^r \circ S_{uex2}^d & \\ & & & S_{22}^r \circ S_{uez2}^d \\ & & & & S_{31}^r \circ S_{uex3}^d \\ & & & & & S_{32}^r \circ S_{uez3}^d \end{bmatrix} \begin{bmatrix} \bar{u}_{ex1} \\ \bar{u}_{ez1} \\ \bar{u}_{ex2} \\ \bar{u}_{ez2} \\ \bar{u}_{ex3} \\ \bar{u}_{ez3} \end{bmatrix}$$

Then the incidence matrix of extendible link \mathbf{H}_e can be given as:

$$\mathbf{H}_e = \begin{bmatrix} \begin{bmatrix} S_1^r \\ S_2^r \\ S_3^r \end{bmatrix}^T \\ \begin{bmatrix} S_1^r \\ S_2^r \\ S_3^r \end{bmatrix}^T \\ \begin{bmatrix} S_1^r \\ S_2^r \\ S_3^r \end{bmatrix}^T \end{bmatrix}^{-1} \begin{bmatrix} S_{11}^r \circ S_{uex1}^d & & & \\ & S_{12}^r \circ S_{uez1}^d & & \\ & & S_{21}^r \circ S_{uex2}^d & \\ & & & S_{22}^r \circ S_{uez2}^d \\ & & & & S_{31}^r \circ S_{uex3}^d \\ & & & & & S_{32}^r \circ S_{uez3}^d \end{bmatrix} \quad (29)$$

$$[\mathbf{h}_e]_{6 \times 6} = \text{diag}(\mathbf{h}_{ei}) \quad i=1, 2, 3 \quad (30)$$

Where S_i^r represents the screw with exchange of the position of linear part and couple part, i.e.,

$$\begin{Bmatrix} S_1^r \\ S_2^r \\ S_3^r \end{Bmatrix} = \begin{Bmatrix} S_{i1}^r \\ S_{i2}^r \end{Bmatrix} = \begin{Bmatrix} 0 & 0 & 0; & -\cos\phi_i & 0 & \sin\phi_i \\ -l_{ei}\sin\phi_i & 0 & -l_{ei}\cos\phi_i; & 0 & 1 & 0 \end{Bmatrix}$$

The compliance matrix C_e caused by the deformation of the extendible link can be obtained by substituting Eqs. (29) and (30) into Eq. (13).

3.3.2 Swing link

When only the deformations of swing link are taken into account, from Eq. (26) the deformation equation of swing link can be expressed as Eq. (31).

$$\{\delta X_s\} = \sum_{j=2,3}^{5,6} q_{ij} S_{ij} + \sum_{k=1}^5 d_{sik} S_{sik}^d \quad \text{for } i=1, 2, 3 \quad (31)$$

Taking the reciprocal product of both sides of Eq. (31) with S_i^r , yields,

$$S_i^r \circ \{\delta X_s\} = \begin{bmatrix} S_{i1}^r \circ S_{usxi}^d & & & & & \\ & S_{i2}^r \circ S_{\theta sxi}^d & & & & \\ & & S_{i3}^r \circ S_{usyi}^d & & & \\ & & & S_{i4}^r \circ S_{\theta syi}^d & & \\ & & & & S_{i5}^r \circ S_{\theta szi}^d & \\ & & & & & S_{i6}^r \circ S_{uszi}^d \end{bmatrix} \begin{bmatrix} \bar{u}_{sxi} \\ \bar{\theta}_{sxi} \\ \bar{u}_{sxi} \\ \bar{\theta}_{sxi} \\ \bar{u}_{sxi} \end{bmatrix} \quad (32)$$

Eq. (32) can be written in matrix form as Eq. (33). Then the incidence matrix of extendible link \mathbf{H}_s can be given as Eq. (34).

$$\begin{bmatrix} S_1^r \\ S_2^r \\ S_3^r \end{bmatrix} \circ \{\delta X_s\} = \begin{bmatrix} S_{11}^r \circ S_{usx1}^d & & & S_{11}^r \circ S_{usz1}^d \\ S_{12}^r \circ S_{\theta x1}^d & S_{12}^r \circ S_{usy1}^d & S_{12}^r \circ S_{\theta z1}^d & \\ & S_{21}^r \circ S_{usx2}^d & & S_{21}^r \circ S_{usz2}^d \\ & S_{22}^r \circ S_{\theta x2}^d & S_{22}^r \circ S_{usy2}^d & S_{22}^r \circ S_{\theta z2}^d \\ & & S_{31}^r \circ S_{usx3}^d & S_{31}^r \circ S_{usz3}^d \\ & & S_{32}^r \circ S_{\theta x3}^d & S_{32}^r \circ S_{usy3}^d & S_{32}^r \circ S_{\theta z3}^d \end{bmatrix}_{6 \times 15} \begin{bmatrix} \bar{u}_{sx1} \\ \bar{\theta}_{sx1} \\ \bar{u}_{sz1} \\ \vdots \\ \bar{u}_{sx2} \\ \bar{\theta}_{sx2} \\ \bar{u}_{sz2} \\ \vdots \\ \bar{u}_{sx3} \\ \bar{\theta}_{sx3} \\ \bar{u}_{sz3} \\ \bar{\theta}_{sz3} \\ \bar{u}_{sz3} \end{bmatrix}_{15 \times 1} \quad (33)$$

$$\mathbf{H}_s = \begin{bmatrix} S_{11}^r \circ S_{usx1}^d & & & S_{11}^r \circ S_{usz1}^d \\ S_{12}^r \circ S_{\theta x1}^d & S_{12}^r \circ S_{usy1}^d & S_{12}^r \circ S_{\theta z1}^d & \\ & S_{21}^r \circ S_{usx2}^d & & S_{21}^r \circ S_{usz2}^d \\ & S_{22}^r \circ S_{\theta x2}^d & S_{22}^r \circ S_{usy2}^d & S_{22}^r \circ S_{\theta z2}^d \\ & & S_{31}^r \circ S_{usx3}^d & S_{31}^r \circ S_{usz3}^d \\ & & S_{32}^r \circ S_{\theta x3}^d & S_{32}^r \circ S_{usy3}^d & S_{32}^r \circ S_{\theta z3}^d \end{bmatrix} \begin{bmatrix} S_1^r \\ S_2^r \\ S_3^r \end{bmatrix} \quad (34)$$

$$[\mathbf{h}_s]_{15 \times 15} = \text{diag}(\mathbf{h}_{si}) \quad i=1, 2, 3 \quad (35)$$

The compliance matrix C_s caused by the deformation of the extendible link can be obtained by substituting Eqs. (34) and (35) into Eq. (13).

According to the former analysis the compliance matrix related to the extendible links C_e and swing links C_s are established, then the global generalized compliance matrix C_G can be obtained based on Eq. (12), and the stiffness modeling of 3-RUPU (C-A) parallel mechanism is accomplished. In the following section, two flexibility indices will be introduced to evaluate the stiffness behavior of the mechanism.

4. Flexibility indices

Conventional stiffness analysis methods, such as stiffness mapping, would require a large number of graphs in order to provide an overview of the stiffness variation. Based on this idea some researchers take the mean value and the standard deviation of a selected parameter as the global flexibility indices [14], but their physical meaning is not clear. Tsai introduced two global flexibility indices which overcome the aforementioned drawback [23]. Similarly, we employ the maximum and minimum singular values of the compliance matrix as flexibility indices to represent the maximum and minimum infinitesimal motions of the platform under unit wrench. The calculation of two flexibility indices can be expressed as Eq. (36).

$$\delta X_{\max} = \max(\sqrt{\text{eign}(C_G^T C_G)}) \quad (36)$$

$$\delta X_{\min} = \min(\sqrt{\text{eign}(C_G^T C_G)})$$

5. Case Study

5.1 Model comparison

To demonstrate the methodology and show the effectiveness, a case study of the mechanism is carried out on the aforementioned 3-RUPU (C-A) parallel mechanism in this section. In the light of the methodology mentioned above, the stiffness analysis is conducted, with structural parameters chosen as follows: the distributed radius of joints on platform and base are respectively $r=50\text{mm}$ and $R=150\text{mm}$; the distributed angle of joints on platform and base are respectively $\theta_1=120^\circ$ the $\theta_2=120^\circ$; the length of the swing link $l_s=50\text{mm}$; the other parameters are set as follows: $E=207\text{Gpa}$, $G=80\text{Gpa}$, $I=4.0 \times 10^4 \text{mm}^4$, $J=2.0 \times 10^4 \text{mm}^4$.

Table 4. Stiffness analysis results of 3-RUPU mechanism.

Analysis model	Analysis results		
	Stiffness in X ($N\text{mm}^{-1}$)	Stiffness in Y ($N\text{mm}^{-1}$)	Stiffness in Z ($N\text{mm}^{-1}$)
Simulation model	382.32	404.58	820.77
FE model	402.73	418.73	862.27
Comparison error	5.33%	3.47%	5.05%

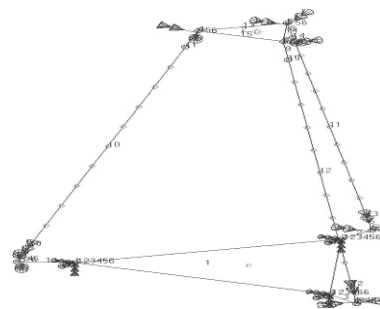


Fig. 7. Finite element model of 3-RUPU mechanism.

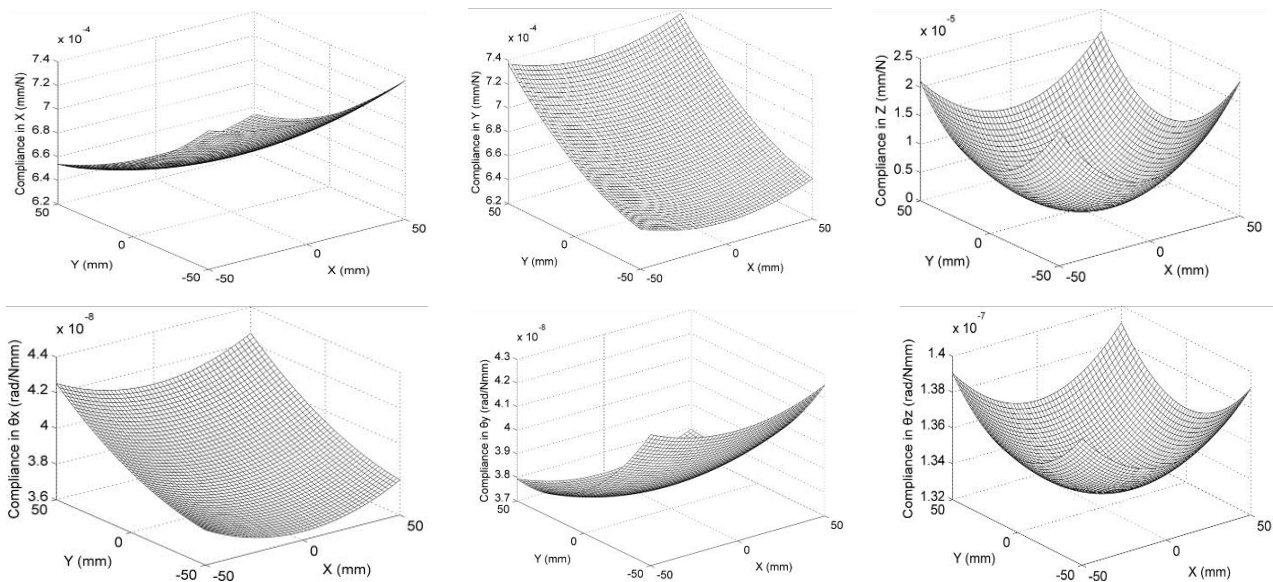


Fig. 8. Stiffness mapping over the x, y cross-section of the workspace.

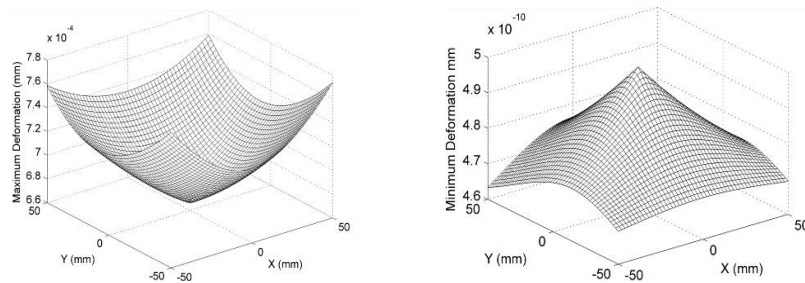


Fig. 9. The maximum and minimum distortions over the XY plane.

A comparative FE model of the 3-RUPU parallel mechanism is set up in MSC/Nastran software as shown in Fig. 7. In the FE model the active joints (R joint and P joint) are fixed, and unit force in x, y and z directions is sequentially applied on mobile platform so that the corresponding deformation can be obtained. Based on the relationship between compliance and stiffness the stiffness of the mechanism can be obtained. The stiffness models of both the simulation model and the FE model of the mechanism in initial status are compared in Table 4. The comparison error between simulation model and FE model is within 6%, so the effectiveness of the analysis method is obvious.

5.2 Stiffness atlas

Based on the above modeling method, the stiffness of the mechanism in six directions can be worked out. Simulation is carried out over x, y cross-section over the workspace, and the six-dimensional atlases of compliance of the mechanism are given in Fig. 8.

Based on the stiffness model the two global flexibility indices are derived. With the two indices, an analysis can be conducted to calculate the deformation of the mechanism over the workspace, and the indices can also be used to evaluate the

compliance or stiffness of the configuration under the payload. Fig. 9 shows the maximum and minimum distortions over the XY plane.

From Fig. 8 and Fig. 9, the stiffness features of 3-RUPU (C-A) mechanism can be obtained; the translational stiffness in x and y directions are dual to each other, and equivalent along the homologous axis; the translational and torsional stiffness in z direction are centrosymmetric with z axis, and have extremum at the central original point; the torsional stiffness in x and y directions are dual to each other; the parallel mechanism has the best stiffness performance around the original point.

6. Conclusions

This paper addresses the stiffness modeling and analysis for a family of 6-DoF parallel mechanisms with configurations of 3-RUPU based on screw theory. The method presented in this paper is characterized by utilizing screw theory as a tool for force analysis and deformation analysis. The deformation model of the component link is described by deformation screws, and the existence of the deformation of the kinematic chain is identified in terms of the relationship between the effective screw and deformation screw. A stiffness model of

the mechanism is constructed by virtue of the duality of kinematics and statics, where the deformation of component links is taken as the infinitesimal input, and the output of the platform is regarded as the corresponding deformation of mechanism. Two flexibility indices are introduced, which refer to the maximum and minimum singular values of compliance matrix, and represent for the maximum and minimum infinitesimal motion of the platform under unit wrench. Based on the two indices we could easily get the extremum of the deformation value of the manipulator over the specified workspace. A case study is presented in the paper; the effectiveness of the method is verified through comparison between the presented model and the finite element model. The screw-theory based stiffness modeling method can be applied to the analysis of general parallel mechanisms with complicated structure.

Acknowledgments

This work is financially supported by the Natural Science Foundation of China (Project No. 50935002, 60875060), State Key Laboratory of Robotics and System (HIT) (Project No: SKLRS200719).

References

- [1] M. Arsenault, R. Boudreau, Synthesis of planar parallel mechanisms while considering workspace, dexterity, stiffness and singularity avoidance. *Mechanical Design of the ASME*. 128 (2006) 69-78.
- [2] X. Kong and C. M. Gosselin, Kinematics and singularity analysis of a novel type of 3-CRR 3-DOF translational parallel manipulator. *Int. J. Robot. Res.* 21 (2002) 791-798.
- [3] C. Gosselin and J. Angeles, Singularity analysis of closed loop kinematic chains, *IEEE Robotics and Automation*. 6 (3) (1991) 281-290.
- [4] V. Gough, Contribution to discussion to papers on research in automobile stability and control and in tire performance, *Proceedings of the Auto. Div. Instn. mech. Engrs.* (1956) 392-398.
- [5] D. Stewart, A Platform with six degrees of freedom, *Proc. Inst. Mech. Eng.* (1965) 371-378.
- [6] L. W. Tsai and F. Tahmasebi, Synthesis and analysis of a new class of six degree-of-freedom parallel minimanipulators, *Journal of Robotic Systems*. 10 (5) (1993) 561-580.
- [7] D. Zlatanov, M. Q. Dai, R. G. Fenton and B. Benhabib, Mechanical design and kinematic analysis of a three-legged six degree-of-freedom parallel manipulator, *Robotics, Spatial Mechanisms, and Mechanical Systems*. 45 (1992) 529-536.
- [8] U. Ebert and C. M. Gosselin, Kinematic Study of a new type of spatial parallel platform mechanism, *ASME Design Engineering Technical Conference, Atlanta*. (1998) 13-16.
- [9] H. J. Yu, Bing Li, J. S. Dai and X. J. Yang, Synthesis and Analysis of parallel-robot based flexible fixture for automobile body assembly, *Proceedings of the Int. Conference on Mech. Trans, Chongqing, China*. (2006) 803-808.
- [10] D. Deblaise, X. Hernot and P. Maurine, A systematic analytical method for PKM stiffness matrix calculation, *Proceedings of IEEE Int. Conference on Robotics and Automation*. (2006) 4219-4213.
- [11] D. Zhang, Z. Bi and B. Li, Design and kinetostatic analysis of a new parallel manipulator, *Robotics and Computer-Integrated Manufacturing*. 25 (2009) 782-791.
- [12] D. Zhang, S. Patel, Z. Gao and Y. Ge, Stiffness control for a 3-DOF parallel robot based machine tools, *IEEE Int. Conf. on Information and Automation*. (2008) 1085-1090.
- [13] C. M. Gosselin, Stiffness mapping for parallel manipulators, *IEEE Trans Robot Autom.* 6 (3) (1990) 377-382.
- [14] D. Zhang, F. F. Xi, C. M. Mechefske and S. Y. T. Lang, Analysis of parallel kinematic machine with kinetostatic modelling method, *Robotics and Computer-Integrated Manufacturing*. 20 (2) (2003) 151-165.
- [15] B. S. El-Khasawneh and P. M. Ferreira, Computation of stiffness and stiffness bounds for parallel link manipulators, *Int J Machine Tools and Manufacture*. 39 (1999) 321-342.
- [16] B. C. Bouzgarrou, J. C. Fauroux, G. Gogu and Y. Heerah, Rigidity analysis of T3R1 parallel robot with uncoupled kinematic, *Proceedings of the 35th Int. Symp. On Robotics, Paris, France*. (2004).
- [17] C. Corradini, J. C. Fauroux, S. Krut and O. Company, Evaluation of a 4 degree of freedom parallel manipulator stiffness, *IFTOMM'2004, Tianjin, China*. (2004) 1857-1861.
- [18] J. S. Przemieniecki, *Theory of Matrix Structural Analysis*, Dover Publications, Inc., New York, (1985).
- [19] H. C. Martin, *Introduction to Matrix Methods of Structural Analysis*, McGraw-Hill Book Company, New York, USA, (1966).
- [20] W. Dong, Z. Du and L. Sun, Stiffness influence atlases of a novel flexure hinge-based parallel mechanism with large workspace, *Proceedings of IEEE ICRA, Barcelona*. (2005) 856-861.
- [21] M. Ceccarelli and G. Carbone, A stiffness analysis for CaPaMan (Cassino Parallel Manipulator), *Mechanism and Machine Theory*. 37 (5) (2002) 427-439.
- [22] T. R. Chandrupatla and A. D. Belegundu, *Introduction to Finite Elements in Engineering* (3rd edition), Prentice Hall, (2002).
- [23] L. W. Tsai, *Robot Analysis: The Mechanics of Serial and Parallel Manipulators*, John Wiley & SONS, New York, USA, (1999).



Bing Li is a PhD and professor at mechanical engineering and currently Head of the Department of Mechanical Engineering and Automation, Shenzhen Graduate School, Harbin Institute of Technology, P. R. China. His research interests include mechanisms and robotics, PKM, sheet metal assembly etc.